eLIFE
elifesciences.org

Figures and figure supplements

Quantitative time-resolved analysis reveals intricate, differential regulation of standard- and immuno-proteasomes

Juliane Liepe, et al.

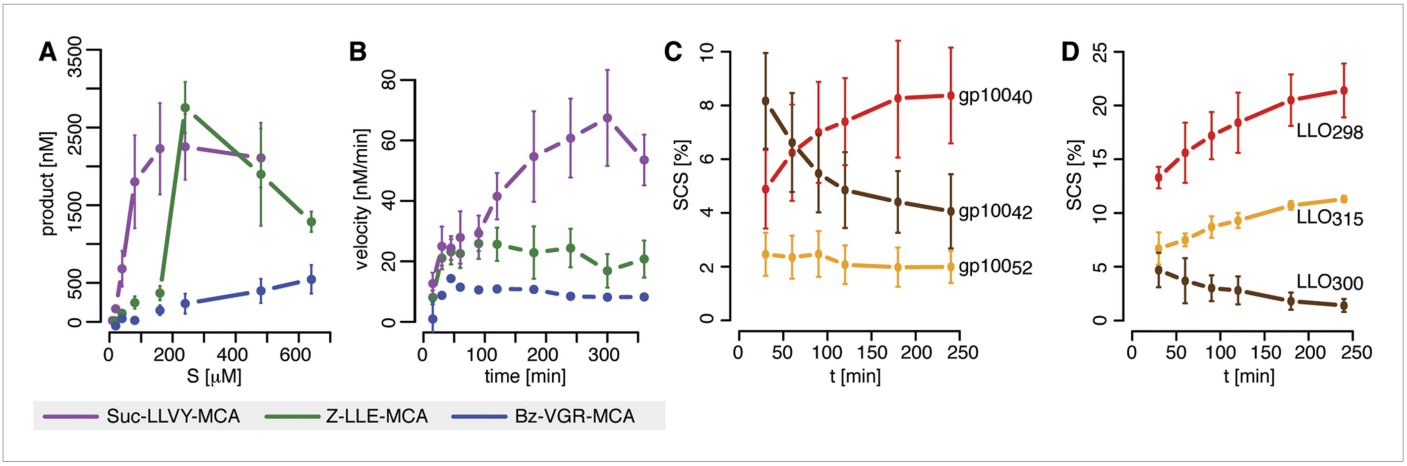

Figure 1. Velocity and specific cleavage site usage by mouse proteasomes varies over time. (**A**) The amount of products generated after 6 hr was measured for different initial substrate concentrations of the short fluorogenic substrates Suc-LLVY-MCA, Bz-VGR-MCA and Z-LLE-MCA by purified 20S mouse liver proteasome. (**B**) The reaction velocity [nM/min] of the same substrates (480 μM) as in (**A**) by purified mouse 20S proteasome was measured over time. (**C**, **D**) Cleavage rate (pmol peptide-bond hydrolysed/[min•mg proteasome]) after the residues $gp100_{40}$ (Arg), $gp100_{42}$ (Lys) and $gp100_{52}$ (Trp) of the synthetic polypeptide $gp100_{35–57}$ (**C**) as well as LLO_{298} (Tyr), LLO_{300} (Arg) and LLO_{315} (Val) of the synthetic polypeptide $LLO_{291–317}$ (**D**) by mouse proteasome. Peptide product amount and site-specific cleavage strength (SCS) was computed by applying QME to each time point of the in vitro kinetics. Values are the mean and the SD of two independent experiments.

DOI: 10.7554/eLife.07545.003

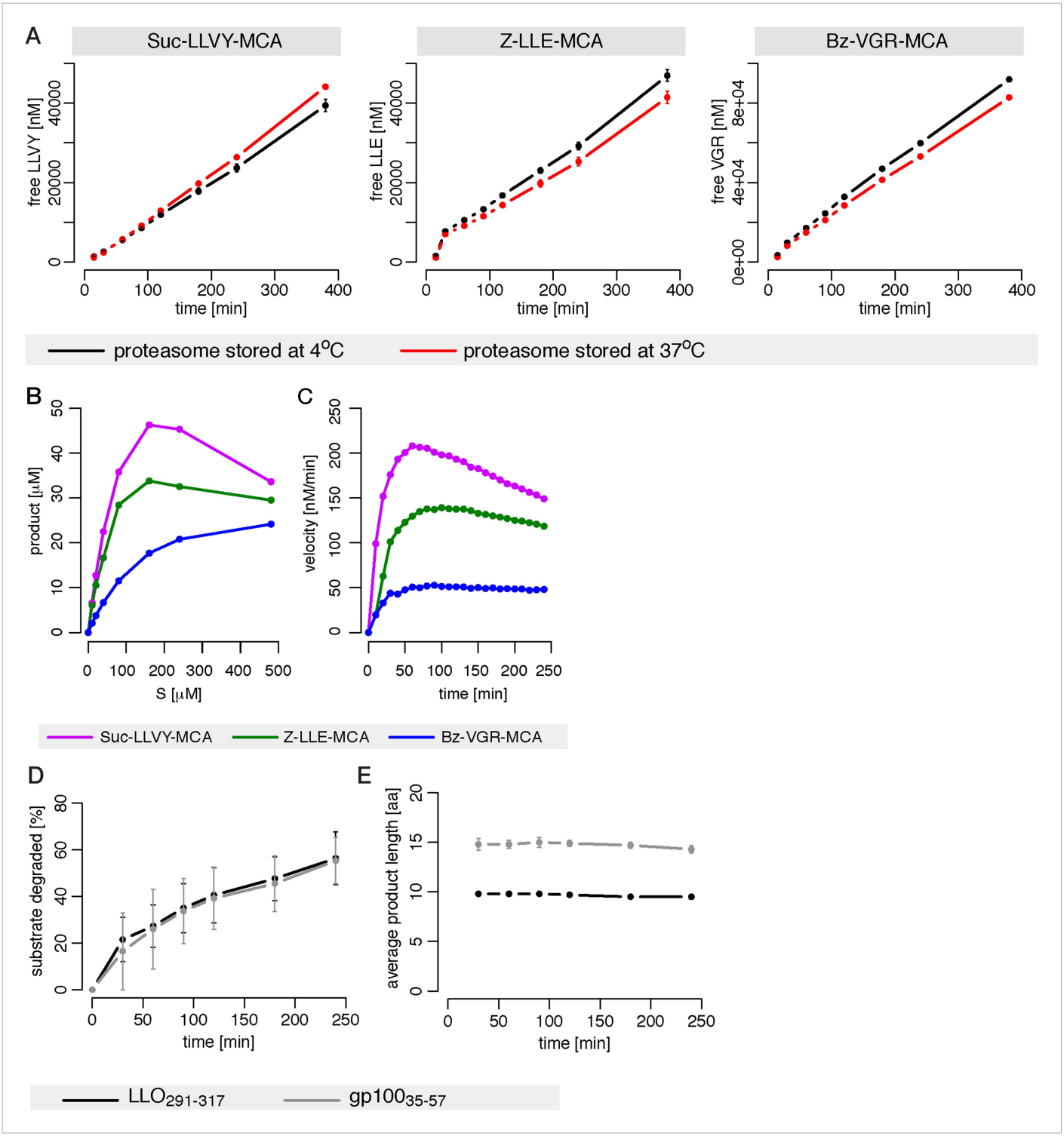

Figure 1—figure supplement 1. Proteasome dynamics are not modified over time because of permanency at 37˚C or product re-entry and further processing. (**A**) Comparison of the degradation rate of the substrates Suc-LLVY-MCA (200 μM), Bz-VGR-MCA (400 μM) and Z-LLE-MCA (400 μM) by 1 μg 20S mouse proteasomes stored prior the assay at 37˚C or 4˚C for 18 hr in the reaction buffer. Means and the SD (bars) of two repeated measurements of a representative assay are shown. (**B**) The amount of product generated after 4 hr was measured for different initial substrate concentrations of the short fluorogenic substrates Suc-LLVY-MCA, Bz-VGR-MCA and Z-LLE-MCA by 5 μg cell protein homogenate. (**C**) The reaction velocity [nM/min] of the same substrates as in (**B**) by 5 μg cell protein homogenate was measured over time. (**D**, **E**) Percentage of substrate cleaved (**D**) and average number of residues

Figure 1—figure supplement 1. continued on next page

Figure 1—figure supplement 1. Continued

of the digestion products (**E**) of the synthetic substrates gp10035–57 and LLO291–317 generated by 1 μg 20S mouse proteasomes. Means and the SD (bars) of two independent experiments are shown.

DOI: 10.7554/eLife.07545.004

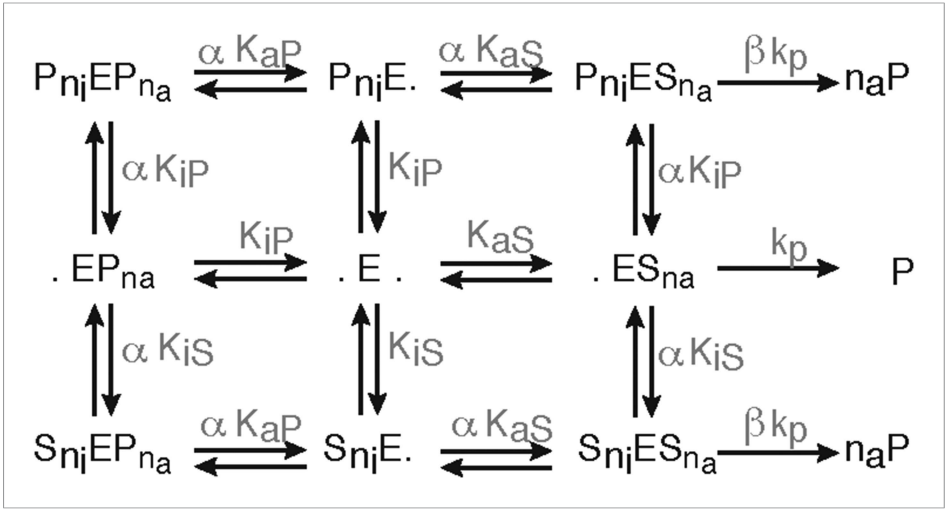

Figure 1—figure supplement 2. Schematic of the substrate inhibition model. Representation of the substrate inhibition model, which is based on the 2-site modifier model originally proposed by ***Schmidtke et al. (2000)***. E denotes the proteasome (enzyme), S denotes the substrate, P denotes the product. S can bind to E and create a substrate-enzyme complex. A dot (.) denotes a free binding site of the proteasome. He substrate and product can bind to the catalytic site (here denoted as a dot on the right side of the E) or to the inhibitory site (here denoted as a dot on the left side of the E) or both. The parameters are defined in ***Figure 2—source data 2***.

DOI: 10.7554/eLife.07545.005

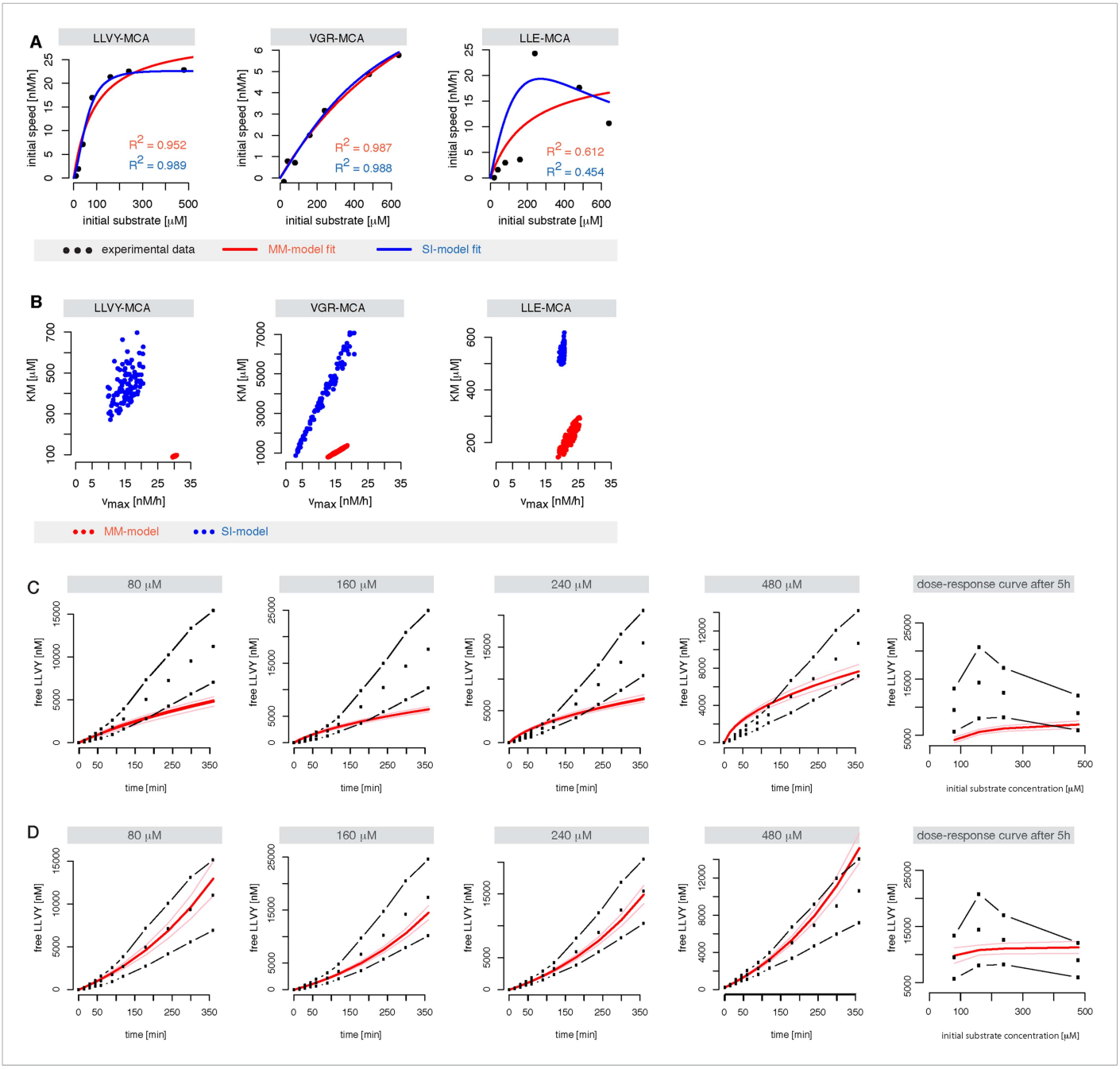

Figure 1—figure supplement 3. Michaelis–Menten and substrate-inhibition models do not describe the short fluorogenic peptide degradation by mouse proteasome. (**A**) Shown are the best possible fits of the MM-model (red) and SI- model (blue) (***Figure 2A,B***, respectively) to the initial cleavage velocities in dependence of the initial substrate concentration. The substrates Suc-LLVY-MCA, Bz-VGR-MCA and Z-LLE-MCA were hydrolysed by mouse proteasome. The initial speed was estimated using linear regression over product concentrations measured at 15, 30, 45 and 60 min. Fits were obtained using ABC-SMC. (**B**) Scatterplot of the kinetic parameters vmax and KM from the inferred posterior parameter distributions of the MM- (red) and SI-model (blue) using the data in (**A**). The point clouds demonstrate the uncertainty in the parameter estimates and their correlations. (**C**, **D**) Shown are the mean (black dots) of two independent experiments (dashed dotted line) of Suc-LLVY-MCA hydrolysis over time. The data were used to calibrate the models in ***Figure 2C,D*** (substrate inhibition model with positive feedback on binding and hydrolysis, respectively). Shown as red line is the mean time course of the calibrated model. Both models fail to represent the experimental data. In vitro digestion of substrate (its concentrations are depicted above each chart) was carried out by mouse proteasome over time. Models are described at ***Figure 2C,D***.

DOI: 10.7554/eLife.07545.006

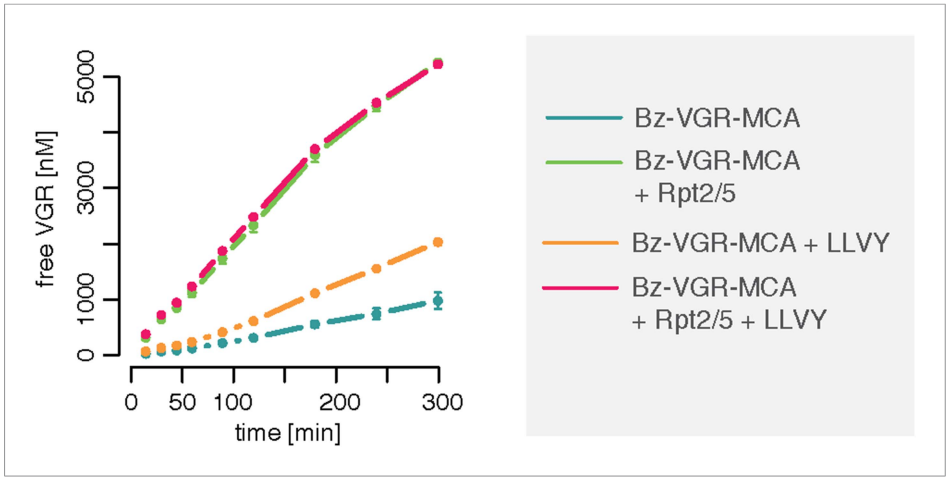

Figure 1—figure supplement 4. Gate opening by Rpt peptides override the enhancing effect mediated by LLVY peptide. Over time cleavage of the substrate Bz-VGR-MCA (200 μM) by 0.25 μg 20S mouse proteasomes in presence of LLVY, Rpt2/5 or LLVY and Rpt2/5 peptides. Means and SD (bars) of repeated measurements (n = 2) of a representative experiment are shown.

DOI: 10.7554/eLife.07545.007

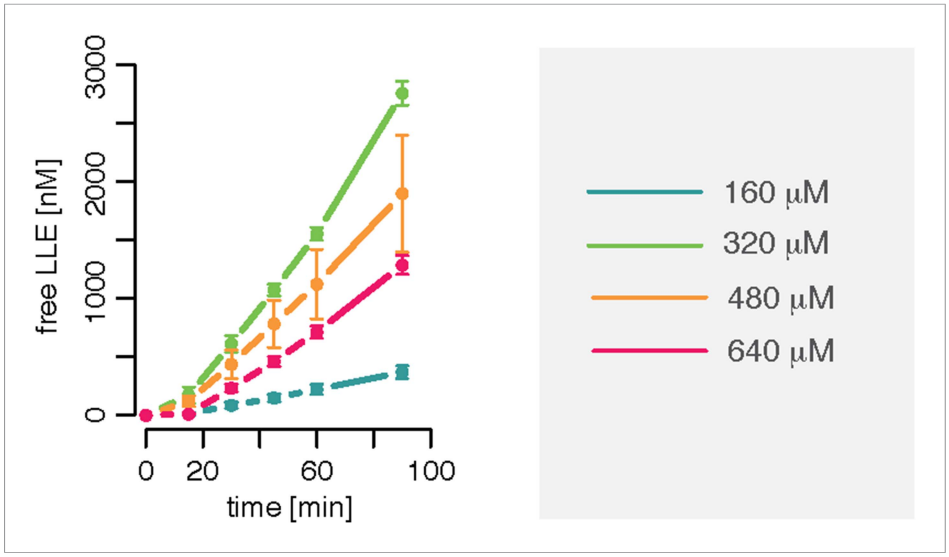

Figure 1—figure supplement 5. Substrate inhibition effect is evident for Z-LLE-MCA degradation kinetics. Amount of products released after cleavage of different concentrations of the substrate Z-LLE-MCA by 0.125 μg 20S mouse protea- some. Means and SD (bars) of two independent experiments are shown.

DOI: 10.7554/eLife.07545.008

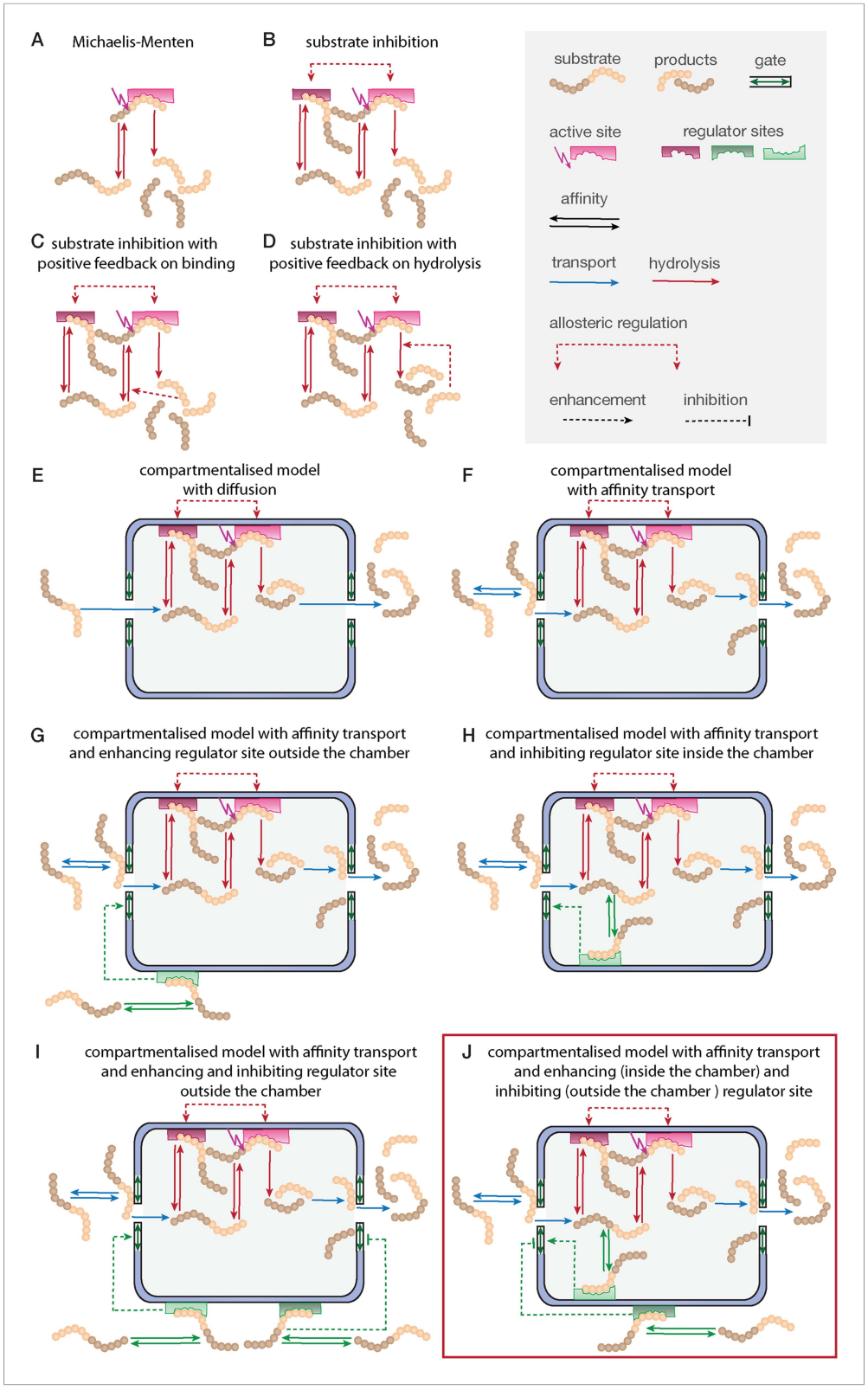

Figure 2. Development of the mathematical model. Schematics of the developed and tested models. Reactions involved in peptide-bond hydrolysis are indicated in red, steps involved in substrate and product transport are indicated in blue and the regulation of the transport is indicated in green. Models in (**A**–**D**) are without the proteasome as a separate compartment, while (**E**–**J**) are compartmentalised models. Note, for simplicity the

Figure 2. continued on next page

Figure 2. Continued

schematics contain only one active site (instead of the two copies for each active site). Furthermore peptides can enter and leave the proteasome chamber through both gates.

DOI: 10.7554/eLife.07545.009

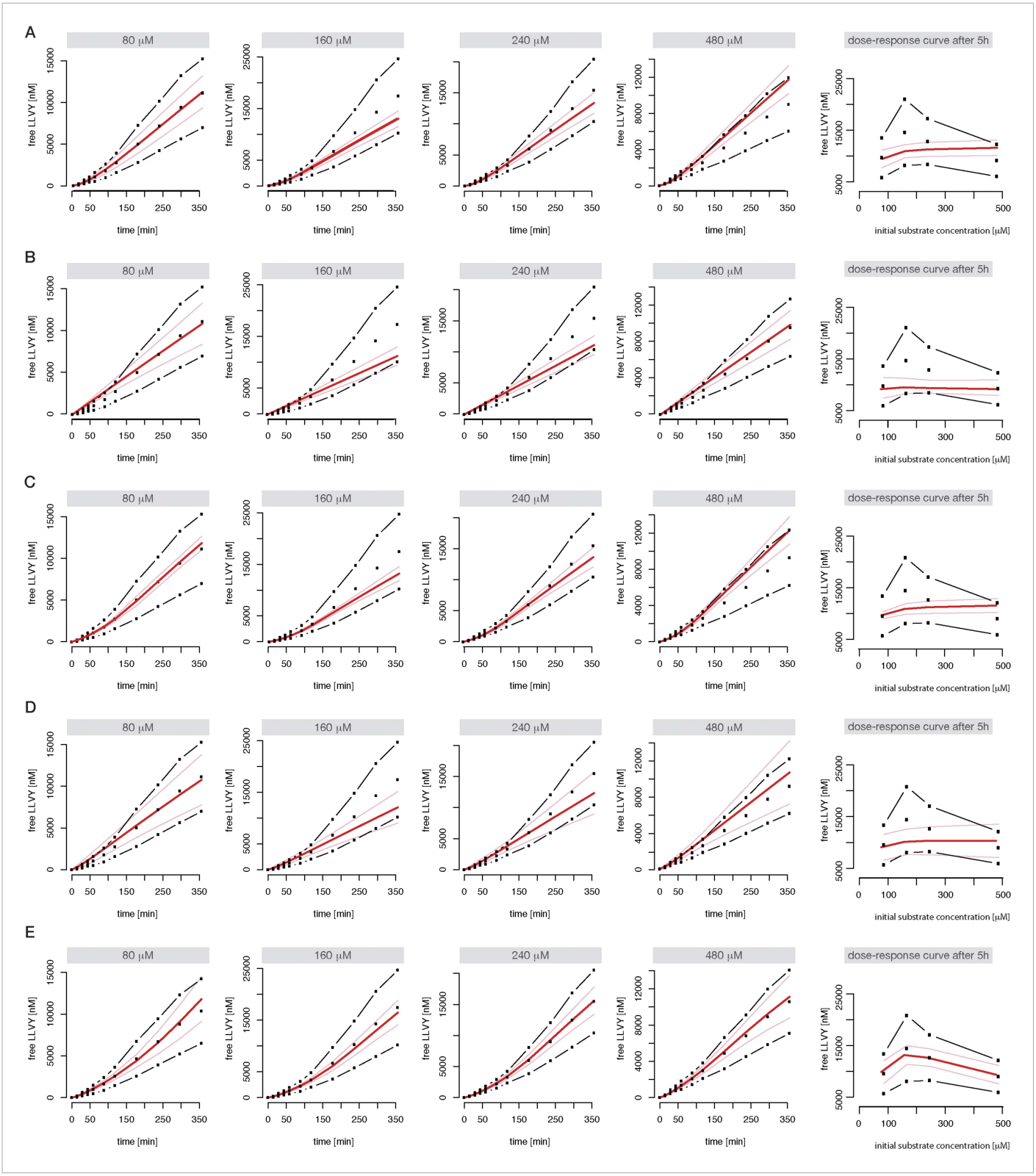

Figure 2—figure supplement 1. Compartmentalised models with affinity transport enhancing regulatory site(s) inside the chamber and substrate inhibitory site(s) best fit the experimental data. Fitting of the Suc-LLVY-MCA cleavage kinetics by compartmentalised models with affinity transport (**A**) and enhancing regulation outside the chamber (**B**), inside the chamber (**C**), enhancing and inhibiting regulation of peptide transport inside the chamber (**D**) or

Figure 2—figure supplement 1. continued on next page

Figure 2—figure supplement 1. Continued

enhancing regulation inside the chamber and inhibiting regulation of transport outside the chamber (**E**). In vitro digestion of substrate (its concentrations are depicted above each chart) was carried out by 0.125 μg 20S mouse proteasome over time. Models are described in ***Figure 2E–J***. Black dashed-dotted lines are two independent experiments, black dots are their means, red and pink lines are the mean and standard deviations of the calibrated model, respectively.

DOI: 10.7554/eLife.07545.013

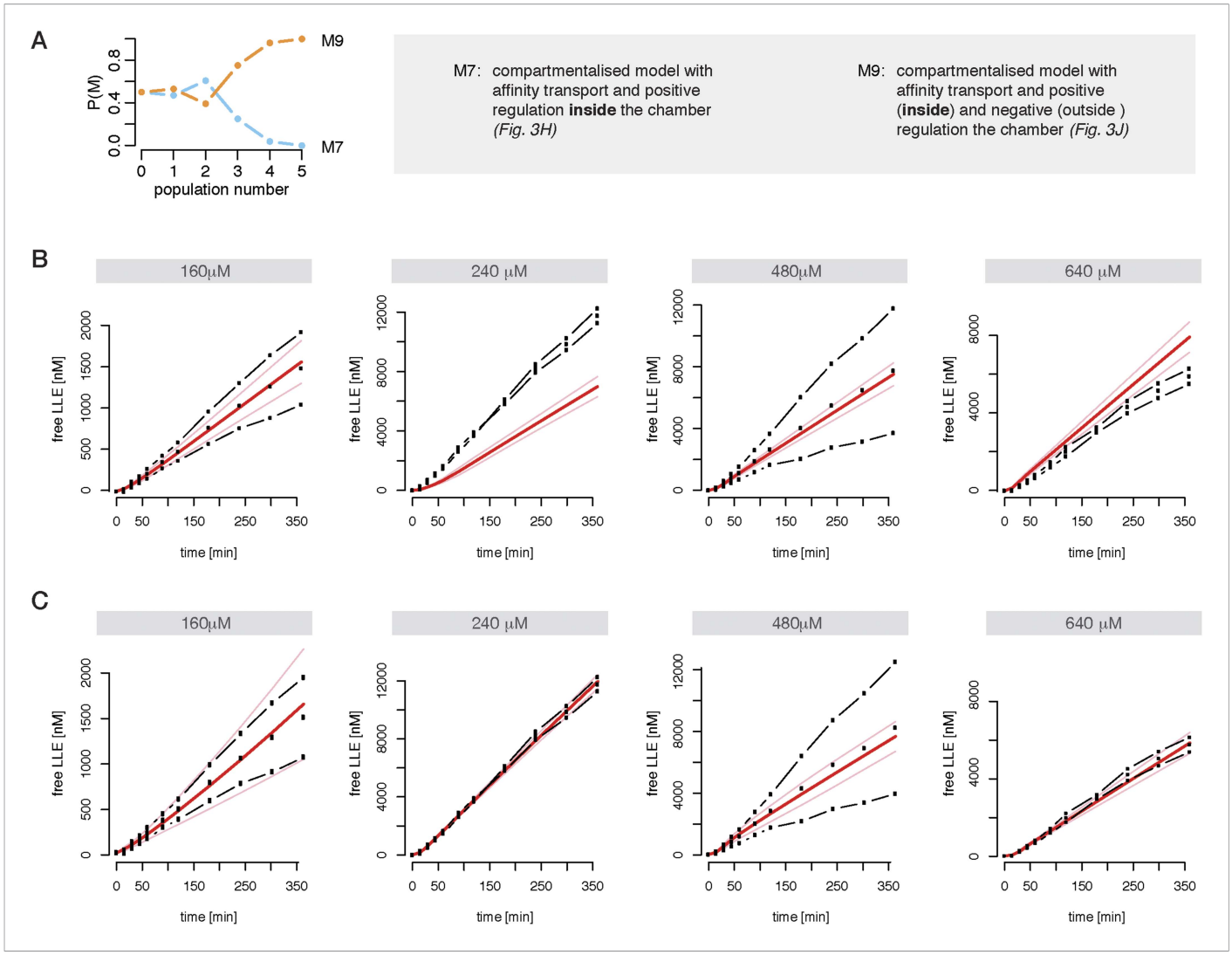

Figure 2—figure supplement 2. Compartmentalised model with affinity transport and enhancing regulatory site(s) inside the chamber and inhibiting site (s) outside the chamber fit the experimental data best. (**A**) Model distributions resulting from Bayesian model selection (ABC-SMC) to discriminate between the models shown in ***Figure 2H,J***. Data used were the cleavage kinetics of the substrate Z-LLE-MCA. (**B**, **C**) Fitting of the Z-LLE-MCA cleavage kinetics by compartmentalised models with affinity transport as well as enhancing regulator site and inhibiting regulator site inside the chamber (**B**) or enhancing regulator site inside the chamber and inhibiting regulator site outside the chamber. In vitro digestion of substrate (its concentrations are depicted above each chart) was carried out by 0.125 μg 20S mouse proteasome over time. Models are described at ***Figure 2H,J***. Black dashed-dotted lines are two independent experiments, black dots are their means, red and pink lines are the mean and standard deviations of the calibrated model, respectively.

DOI: 10.7554/eLife.07545.014

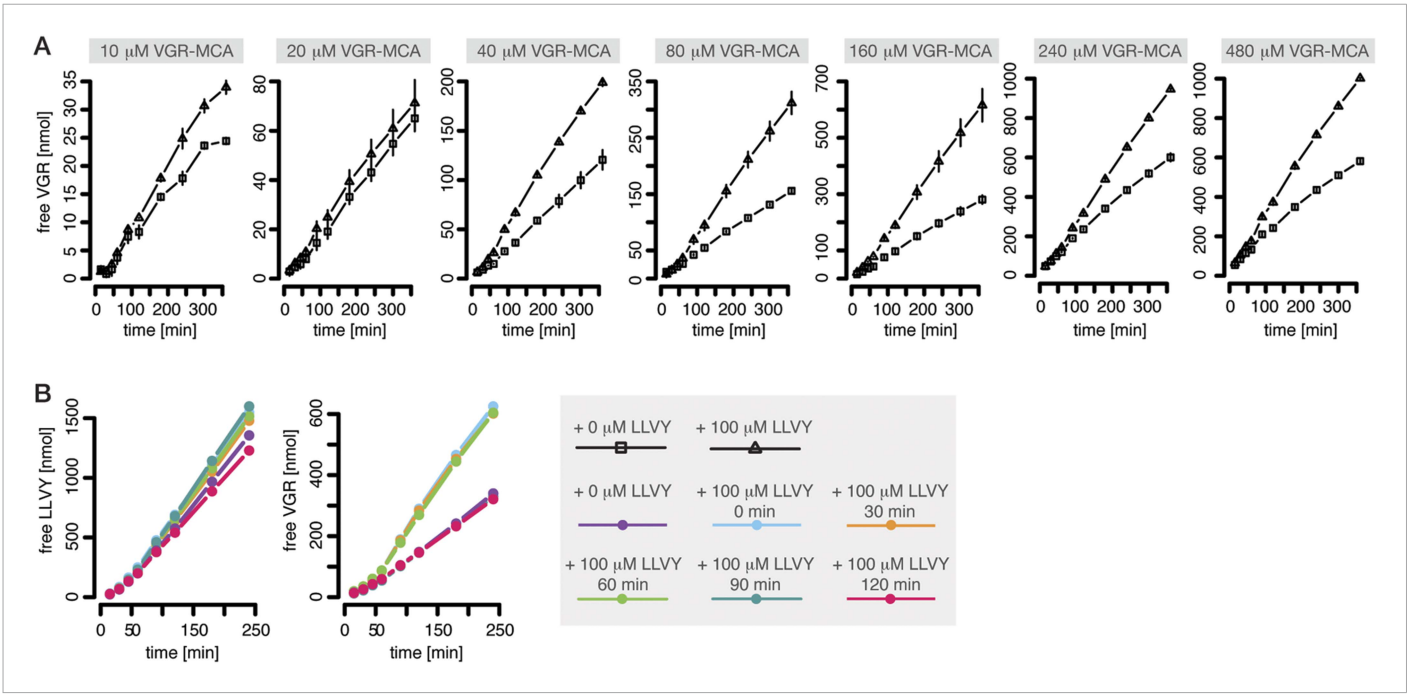

Figure 3. Peptide-mediated enhancement of proteasome activity. (**A**) Product formation over time from degradation of Bz-VGR-MCA by mouse proteasome in presence or absence of LLVY peptide over time. (**B**) Product formation from degradation of Suc-LLVY-MCA and Bz-VGR-MCA (100 μM and 200 μM, respectively) after pre-incubation at 37˚C of mouse proteasome with LLVY peptide over time.

DOI: 10.7554/eLife.07545.015

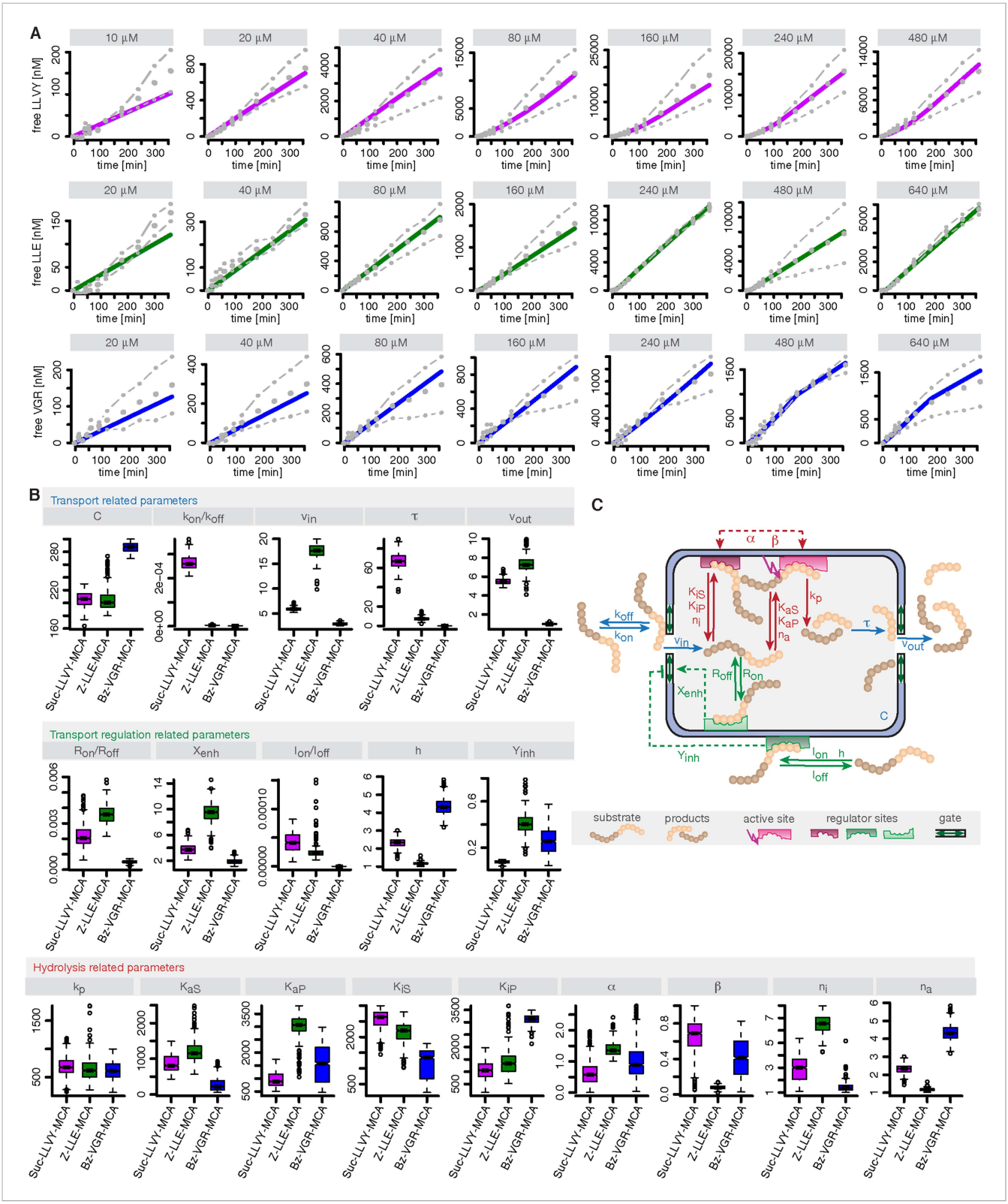

Figure 3—figure supplement 1. Compartmentalised model with affinity transport and enhancing regulatory site(s) inside the chamber and substrate inhibitory site(s) outside the chamber and its kinetic parameters. (**A**) Model fits of the Suc-LLVY-MCA (purple lines), Bz-VGR-MCA (blue lines) and Z-LLE-MCA (green lines) cleavage dynamics by the compartmentalised model with affinity transport as well positive regulation inside the chamber and negative

Figure 3—figure supplement 1. continued on next page

Figure 3—figure supplement 1. Continued

regulation outside the chamber to the mean (grey dots) of two independent experiments (dashed dotted lines). In vitro digestion of substrate (its concentrations are depicted above each chart) was carried out by 0.125 μg 20S mouse proteasome over time. (**B**) Estimated model parameters related to transport, transport regulation and hydrolysis resulting from the degradation kinetics of the substrates Suc-LLVY-MCA, Bz-VGR-MCA and Z-LLE-MCA by 0.125 μg 20S mouse proteasome. The colours correspond to the colours in (**A**). (**C**) Schematic of the compartmentalised model with affinity transport as well positive regulation inside the chamber and negative regulation outside the chamber and the associated model parameters. Transport related reactions are depicted in blue, transport regulation reactions are depicted in green, hydrolysis and hydrolysis regulation related reactions are depicted in red.

DOI: 10.7554/eLife.07545.016

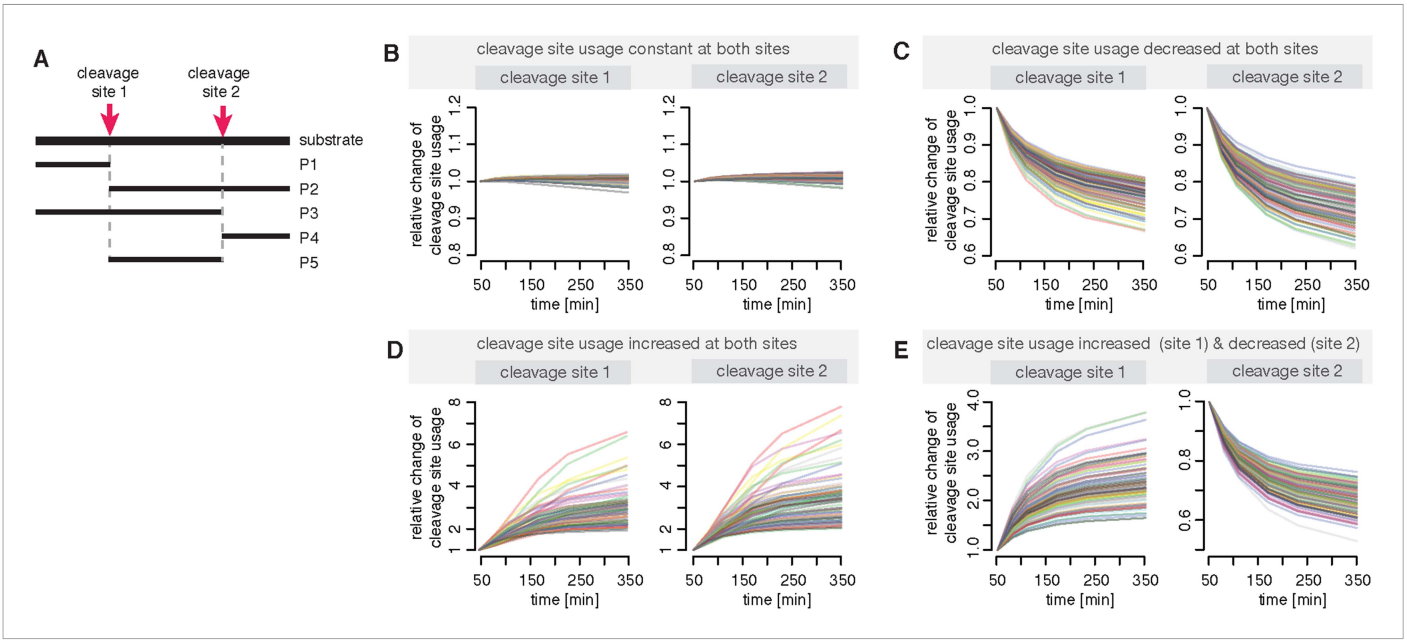

Figure 3—figure supplement 2. Compartmentalised model with affinity transport and enhancing regulatory site(s) inside the chamber and substrate inhibitory site(s) outside the chamber can simulate the different dynamics of polypeptides cleavage sites as observed in in vitro digestions. (**A**) Schematic of the hypothetical substrate with two cleavage sites and the possible resulting products. (**B**–**E**) Shown is the relative change of the cleavage site usage for cleavage site 1 and cleavage site 2 based on in silico simulations of the polypeptide model with randomly sampled parameters. We used ABC-SMC for experimental design (***Liepe et al., 2013***) in order to allow no change in the relative cleavage site usage (**B**), a decrease of the relative cleavage site usage for both sites (**C**), an increase of the relative cleavage site usage for both sites (**D**) or an increase at site 1 and a decrease at site 2 in the relative cleavage site usage (**E**).

DOI: 10.7554/eLife.07545.017

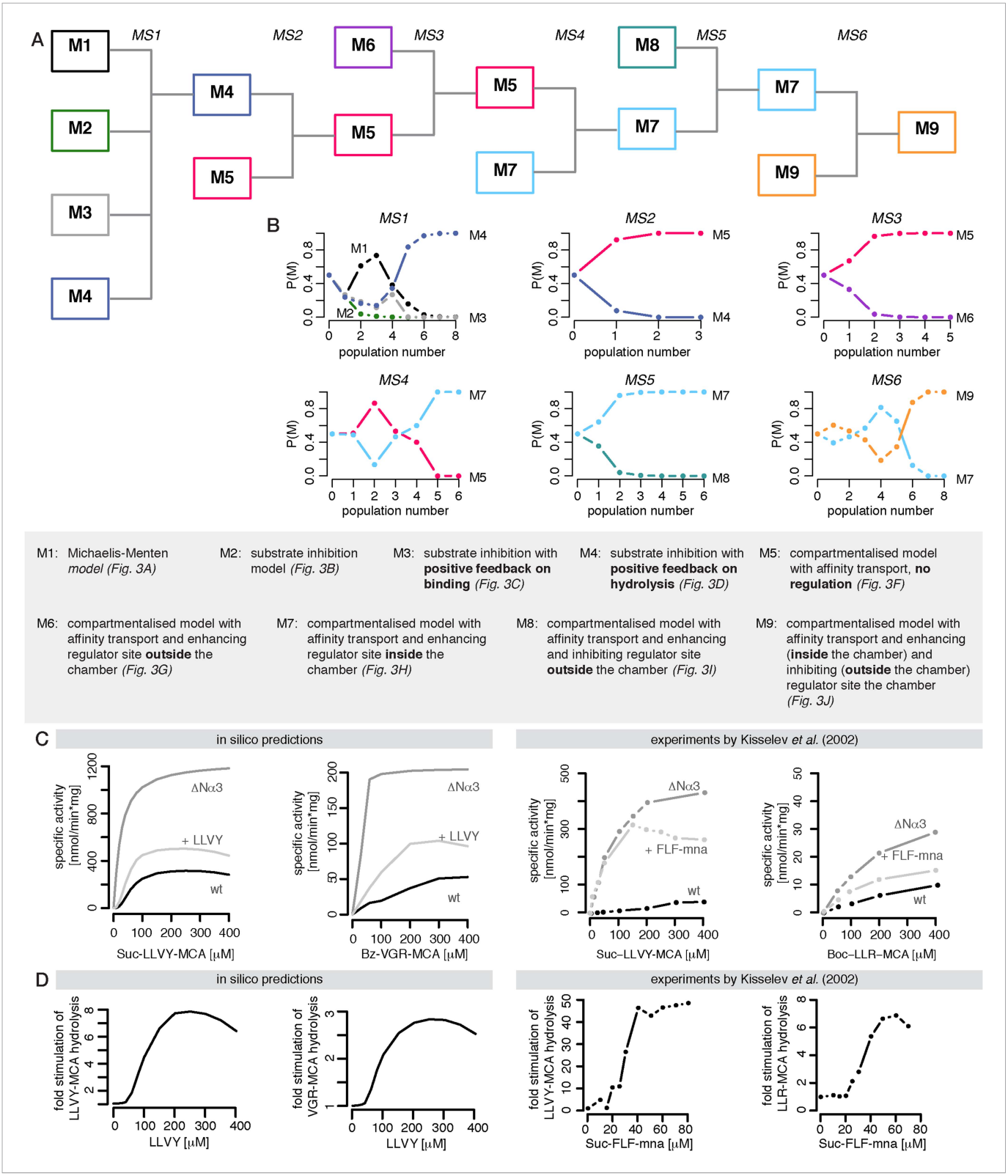

M1: Michaelis-Menten *model (Fig. 3A)*

M2: substrate inhibition model *(Fig. 3B)*

M3: substrate inhibition with **positive feedback on binding** *(Fig. 3C)*

M4: substrate inhibition with **positive feedback on hydrolysis** *(Fig. 3D)*

M5: compartmentalised model with affinity transport, **no regulation** *(Fig. 3F)*

M6: compartmentalised model with affinity transport and enhancing regulator site **outside** the chamber *(Fig. 3G)*

M7: compartmentalised model with affinity transport and enhancing regulator site **inside** the chamber *(Fig. 3H)*

M8: compartmentalised model with affinity transport and enhancing and inhibiting regulator site **outside** the chamber *(Fig. 3I)*

M9: compartmentalised model with affinity transport and enhancing (**inside** the chamber) and inhibiting (**outside** the chamber) regulator site the chamber *(Fig. 3J)*

Figure 4. Bayesian model selection and model validation. (**A**) A model comparison scheme is applied to identify the best candidate among models represented in ***Figure 2F–J***. *MS* stands for model selection. (**B**) The prior model probability is 0.5 for all pairwise model comparisons, and 0.25 for the comparison of models 1–4. The model selection scheme proceeds over SMC populations (***Toni et al., 2009***) each of them returns an updated model probability, until the winning model has a probability of 1 in all comparisons. The colours correspond to (**A**). The winning model is challenged by in silico

Figure 4. continued on next page

Figure 4. Continued

experiments. (**C**) The posterior parameter distributions inferred from a data set using mouse proteasome (***Figure 3—figure supplement 1A–C***) are used to simulate the mean behaviour of opened-gate mutant (ΔNα3) and the effect of Suc-LLVY-MCA. Simulation of the mutant (ΔNα3) is achieved by increasing the parameters v_{in} and v_{out} 10-fold. The model is extended to simulate the effect of the molecule Suc-LLVY-MCA, parameters are taken from the posterior parameter distribution obtained from digestions of Suc-LLVY-MCA. (**D**) Dose response curves are simulated for the effect of the molecule Suc-LLVY-MCA on the peptide-bond hydrolysis of Suc-LLVY-MCA and Bz-VGR-MCA. In (**C**) and (**D**) the results are qualitatively comparable to the results of the experiment by ***Kisselev et al. (2002)***.

DOI: 10.7554/eLife.07545.018

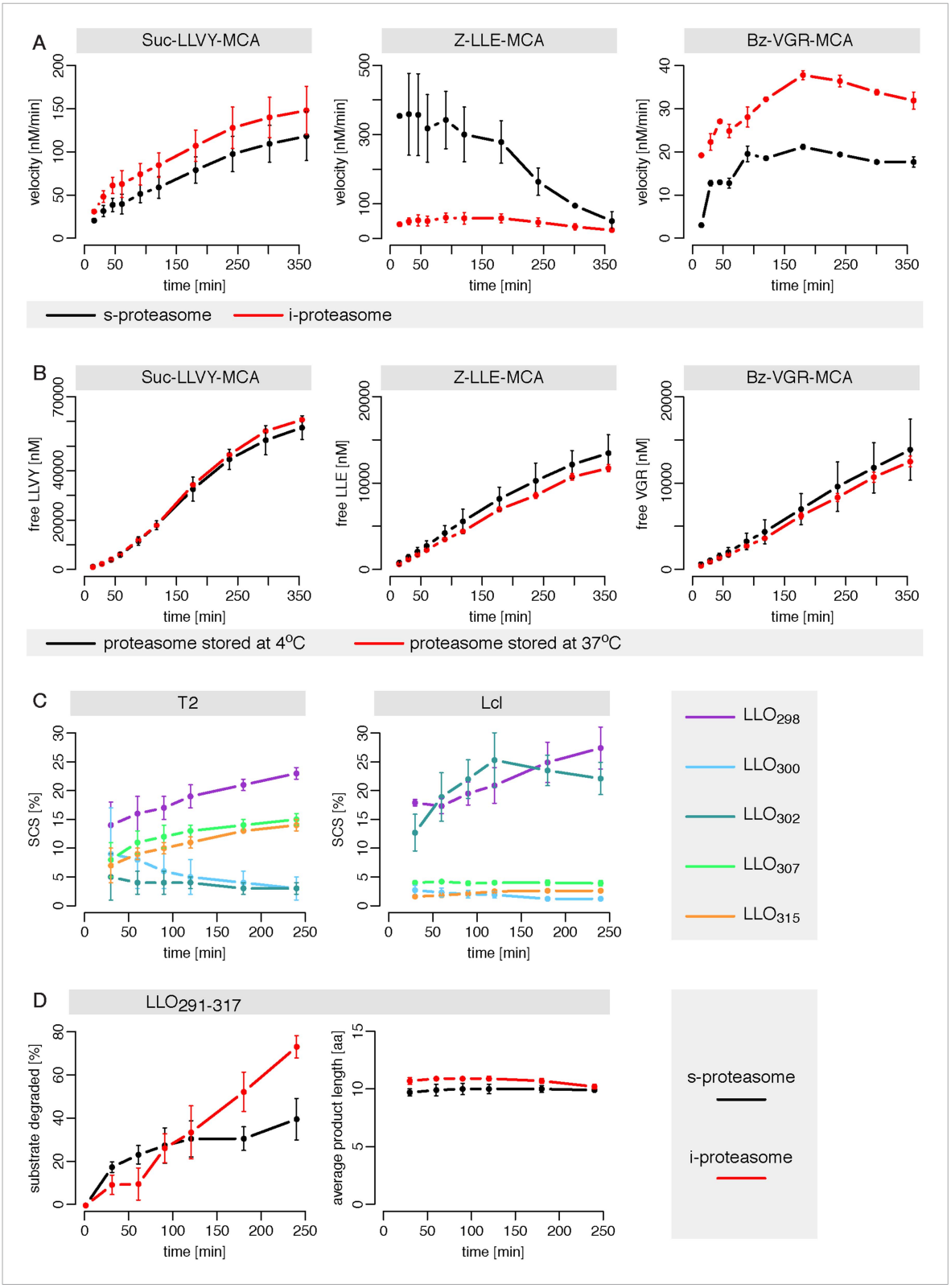

Figure 4—figure supplement 1. Human standard- and immuno-proteasomes vary their cleavage activities over time. (**A**) Cleavage velocity of T2 and LcL 20S proteasomes for the substrates Suc-LLVY-MCA, Bz-VGR-MCA and Z-LLE-MCA over time. (**B**) Comparison of the degradation rate of the substrates Suc-LLVY-MCA (200 μM), Bz-VGR-MCA (400 μM) and Z-LLE-MCA (400 μM) by LcL proteasomes stored prior the assay at 37˚C or 4˚C for 18 hr in the reaction

Figure 4—figure supplement 1. continued on next page

Figure 4—figure supplement 1. Continued

buffer. (**C**) Substrate SCS for the residues Tyr_{298}, Arg_{300}, Val_{302}, Ser307 and Val315 of the synthetic polypeptide LLO291–317 by T2 and LcL proteasomes over time. (**D**) Percentage of substrate cleaved and average number of residues (aa) of the digestion products of the synthetic substrate LLO291–317 generated by T2 and LcL proteasomes. In **A**–**D**, means and the SD (bars) of two independent experiments are shown. (**A**) Cleavage velocity of T2 and LcL 20S proteasomes for the substrates Suc-LLVY-MCA, Bz-VGR-MCA and Z-LLE-MCA over time. (**B**) Comparison of the degradation rate of the substrates Suc- LLVY-MCA (200 μM), Bz-VGR-MCA (400 μM) and Z-LLE-MCA (400 μM) by LcL proteasomes stored prior the assay at 37˚C or 4˚C for 18 hr in the reaction buffer. (**C**) Substrate SCS for the residues Tyr_{298}, Arg_{300}, Val_{302}, Ser307 and Val315 of the synthetic polypeptide LLO291–317 by T2 and LcL proteasomes over time. (**D**) Percentage of substrate cleaved and average number of residues (aa) of the digestion products of the synthetic substrate LLO291–317 generated by T2 and LcL proteasomes. In **A**–**D**, means and the SD (bars) of two independent experiments are shown.

DOI: 10.7554/eLife.07545.019

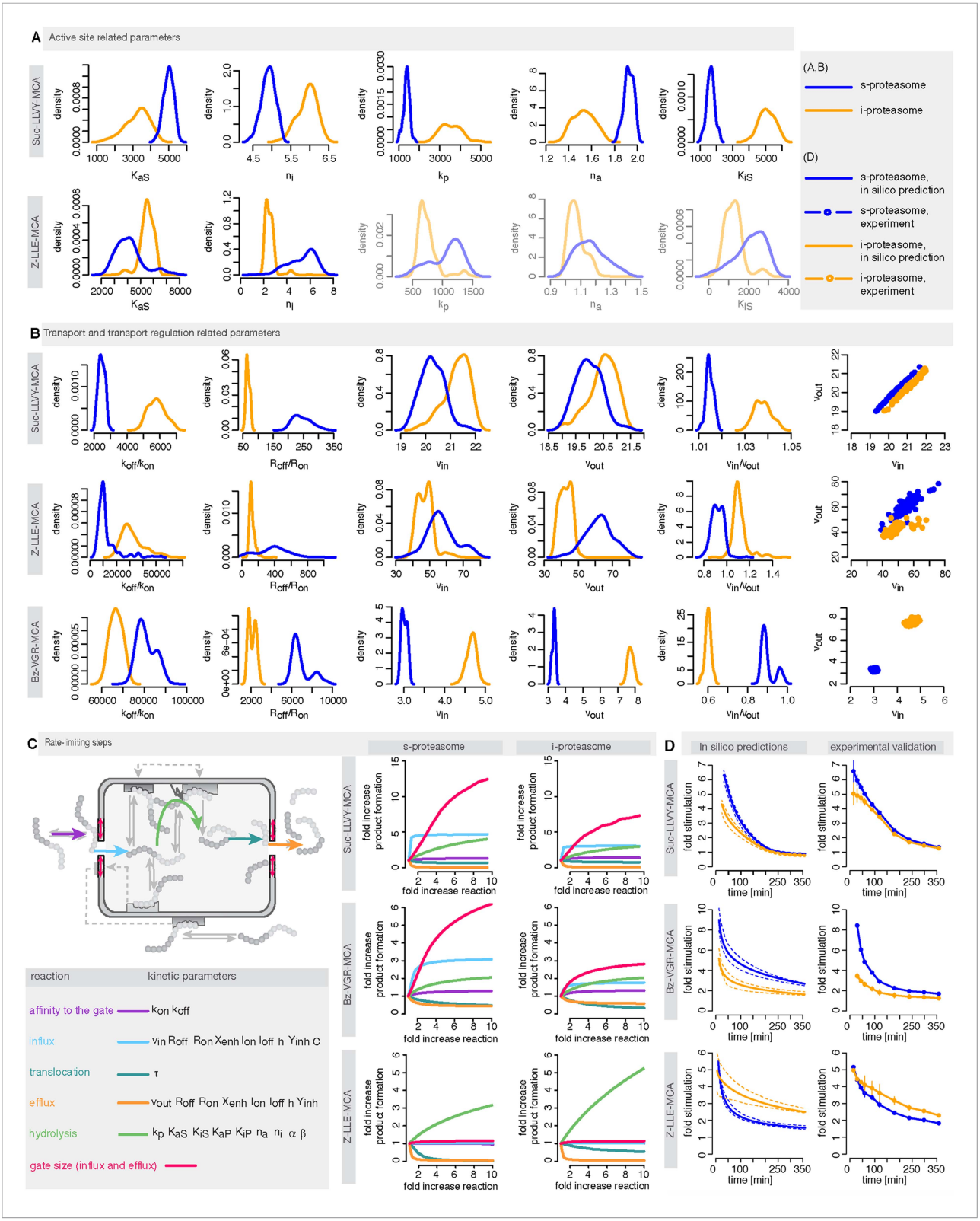

Figure 5. Human s- vs i-proteasomes. (**A**) Marginal posterior parameter distributions for active site related parameters that differ between s- and i-proteasomes. No evidence for differences related to Bz-VGR-MCA was detected. (**B**) Marginal posterior parameter distributions for transport related parameters that differ between s- and i-proteasomes. (**C**) Analysis of rate limiting steps in s- and i-proteasome. Shown is the fold increase of product formation upon increase of a specific reaction. Substrate concentration is 320 μM, measurement is taken after 60 min reaction. (**D**) In silico predictions for

Figure 5. continued on next page

Figure 5. Continued

fold stimulation of substrate hydrolysis in presence of Rpt peptides and experimental validation. A final concentration of 40 μM Rpt peptides was added to the standard experimental setup described in 'Materials and methods'. Dashed lines indicate 5%- and 95%-iles of the predictions.

DOI: 10.7554/eLife.07545.020

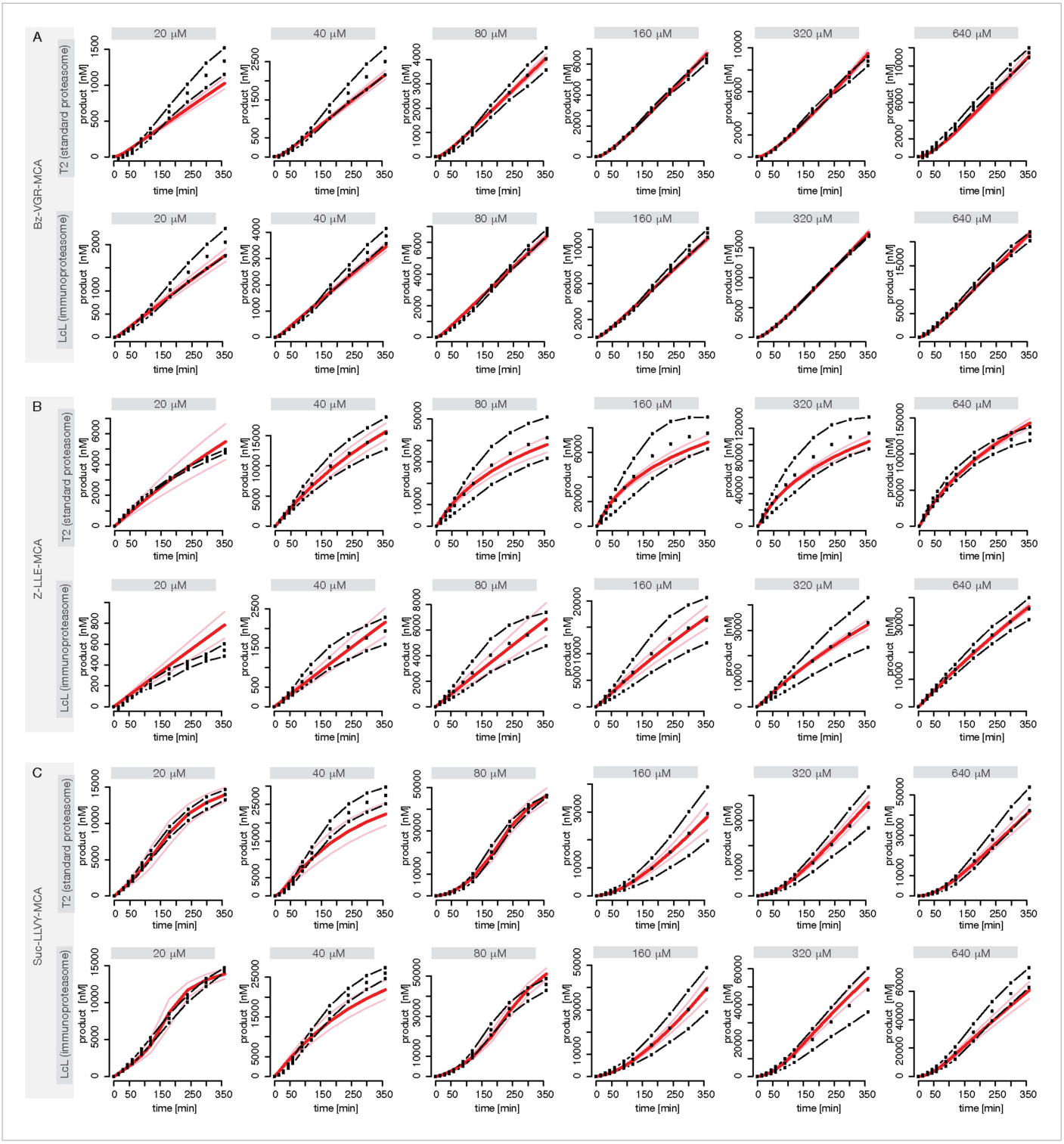

Figure 5—figure supplement 1. Fitting of experimental data using the compartmentalised models with affinity transport en- hancing regulatory site(s) inside the chamber and substrate inhibitory site(s). (**A**–**C**) Fitting of the Suc-LLVY-MCA (**A**), Bz-VGR-MCA (**B**) and Z-LLE-MCA (**C**) cleavage kinetics. In vitro digestion of substrate (its concentrations are depicted above each chart) was carried out by 0.5 μg 20S T2 and LcL human proteasomes, respectively, over time. The model is described at ***Figure 2J***. Black dashed-dotted lines are two independent experiments, black dots are their means, red and pink lines are the mean and standard deviations of the calibrated model, respectively.

DOI: 10.7554/eLife.07545.021

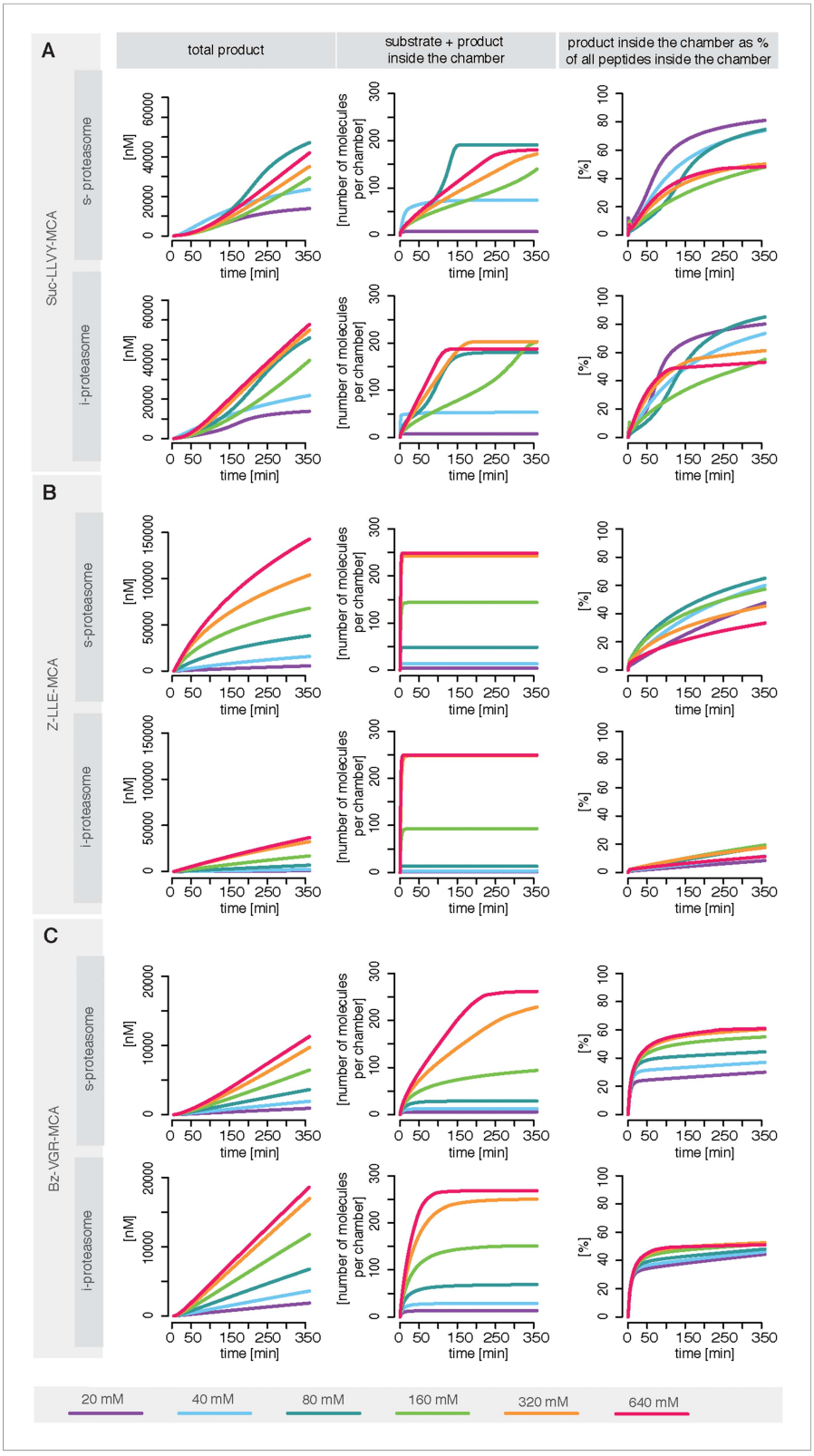

Figure 6. Rate limiting steps of human proteasome activity. The mean of in silico predictions (coloured lines) is plotted over time for the degradation of the substrates Suc-LLVY-MCA (**A**), Z-LLE-MCA (**B**) and Bz-VGR-MCA (**C**) with varying initial substrate concentrations using human s- and i-proteasomes, respectively. The inferred posterior parameter distributions of each substrate were used to simulate the number of peptide molecules (product and

Figure 6. continued on next page

Figure 6. Continued

substrate) and the relative amount of product vs total amount of peptides inside the chambers over time.
DOI: 10.7554/eLife.07545.022

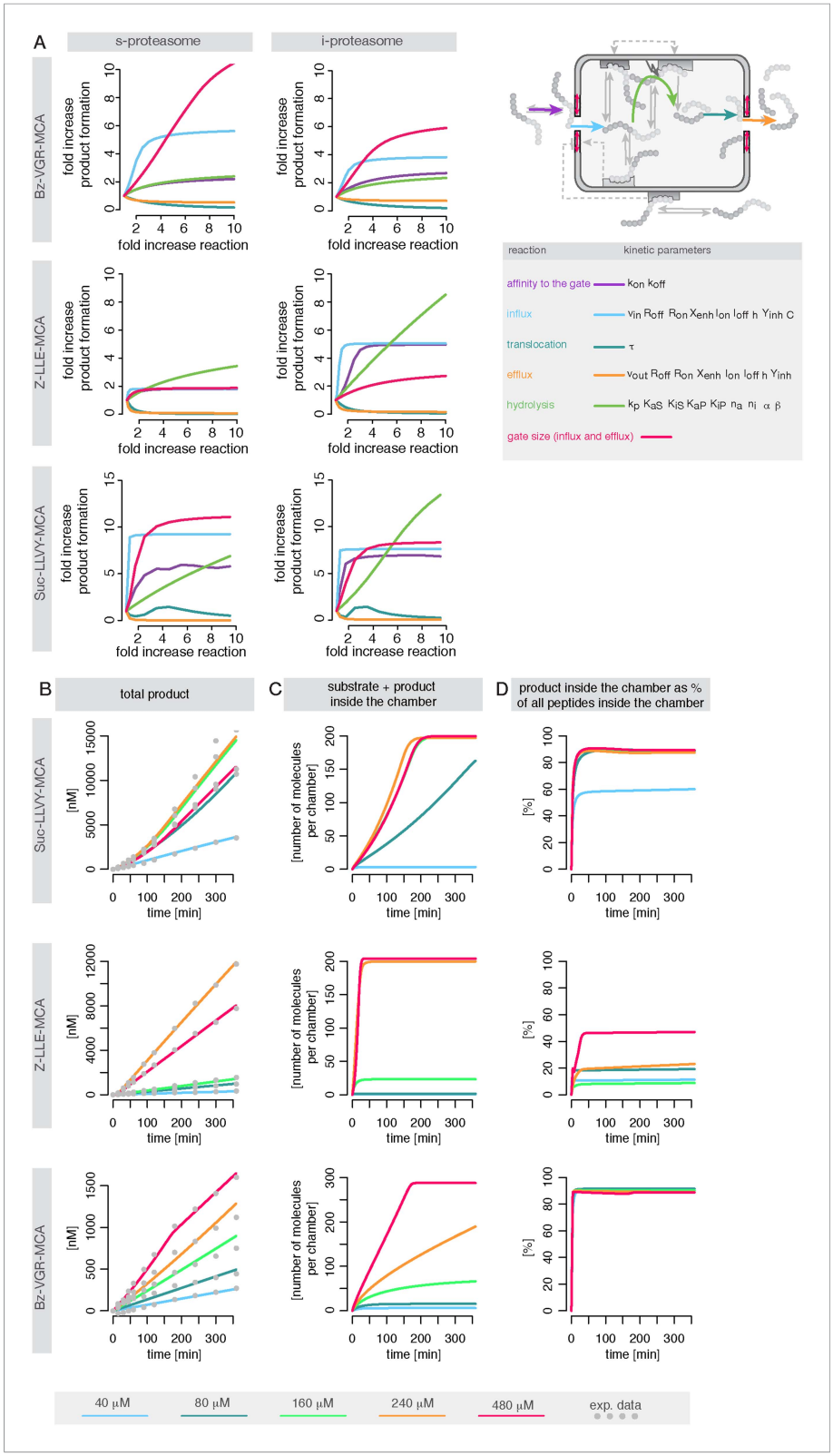

Figure 6—figure supplement 1. Rate limiting steps of proteasome peptide degradation. (**A**) In silico analysis of rate-limiting steps in human s- and i-proteasome. Shown is the fold increase of product formation upon increase of a specific reaction. Substrate concentration is 80 μM, measurement is taken after 60 min reaction. The reaction that

Figure 6—figure supplement 1. continued on next page

Figure 6—figure supplement 1. Continued

increases the product formation strongest indicates the rate-limiting step. (**B**) The mean of experimental data (grey dots) and the mean of simulated fits (coloured lines) is plotted over time for the degradation of Suc-LLVY-MCA, Bz-VGR-MCA and Z-LLE-MCA by mouse proteasome with varying initial substrate concentrations. (**C**) The inferred posterior parameter distributions of each substrate were used to simulate the mean behaviour of the number of peptide molecules (product and substrate) inside each proteasome chamber over time. (**D**) The relative amount of product compared to total amount of peptides inside the chamber over time resulting from the simulations is shown.

DOI: 10.7554/eLife.07545.023